



OPEN

Low dose rifaximin combined with *N*-acetylcysteine is superior to rifaximin alone in a rat model of IBS-D: a randomized trial

Gabriela Leite¹, Ali Rezaie^{1,2}, Walter Morales¹, Stacy Weitsman¹, Juliana de Freitas Germano¹, Gillian M. Barlow¹, Gonzalo Parodi¹, Maya L. Pimentel¹, Maria Jesus Villanueva-Millan¹, Maritza Sanchez¹, Sarah Ayyad¹, Ruchi Mathur^{1,3} & Mark Pimentel^{1,2}✉

Rifaximin is FDA-approved for treatment of irritable bowel syndrome with diarrhea (IBS-D), but poor solubility may limit its efficacy against microbes in the mucus layer, e.g. *Escherichia coli*. Here we evaluate adding the mucolytic *N*-acetylcysteine (NAC) to improve rifaximin efficacy. In a resazurin checkerboard assay, combining rifaximin with NAC had significant synergistic effects in reducing *E. coli* levels. The optimal rifaximin + NAC combination was then tested in a validated rat model of IBS-D (induced by cytolethal distending toxin [CdtB] inoculation). Rats were inoculated with vehicle and treated with placebo (Control-PBS) or rifaximin + NAC (Control-Rif + NAC, safety), or inoculated with CdtB and treated with placebo (CdtB-PBS), rifaximin (CdtB-Rifaximin), or rifaximin + NAC (CdtB-Rif + NAC) for 10 days. CdtB-inoculated rats (CdtB-PBS) developed wide variability in stool consistency ($P = 0.0014$) vs. controls (Control-PBS). Stool variability normalized in rats treated with rifaximin + NAC (CdtB-Rif + NAC) but not rifaximin alone (CdtB-Rifaximin). Small bowel bacterial levels were elevated in CdtB-PBS rats but normalized in CdtB-Rif + NAC but not CdtB-Rifaximin rats. *E. coli* and *Desulfovibrio* spp levels (each associated with different IBS-D microtypes) were also elevated in CdtB-inoculated (CdtB-PBS) but normalized in CdtB-Rif + NAC rats. Cytokine levels normalized only in CdtB-Rif + NAC rats, in a manner predicted to be associated with reduced diarrhea driven by reduced *E. coli*. These findings suggest that combining rifaximin with NAC may improve the percentage of IBS-D patients responding to treatment.

Keywords Irritable bowel syndrome, Diarrhea-predominant, Rifaximin, *N*-acetylcysteine, Rat model, Bacterial overgrowth, *Escherichia coli*, *Desulfovibrio*

While the pathophysiology of irritable bowel syndrome (IBS) is still incompletely understood, there is growing evidence for a role for the intestinal microbiome¹. This is supported by data demonstrating the beneficial effects of the non-absorbable antibiotic, rifaximin, in treating IBS with diarrhea (IBS-D)². However, only 44% of IBS-D patients met FDA responder endpoints in the TARGET 3 trial³, suggesting either that only part of the pathophysiology of IBS is microbiome based, or that rifaximin alone incompletely treats the microbial causes of IBS-D.

There are multiple theories as to how the microbiome is affected in IBS. Both breath testing and culture data now demonstrate that small intestinal bacterial overgrowth (SIBO), which can be diagnosed based on a positive hydrogen (H_2) breath test, is common in IBS⁴. In fact, clinical guidelines suggest that the cumulative evidence supports the identification of SIBO in IBS^{5,6}, and even more recently, the first global IBS guidelines suggest that SIBO should be screened for in IBS-D⁷. SIBO and IBS-D are now more clearly understood than ever before, with a recent study in human subjects (which for the first time combined breath testing, microbial sequencing, and gastrointestinal symptoms) indicating that IBS-D is associated with two microtypes, one with elevated H_2 on

¹Medically Associated Science and Technology Program, Cedars-Sinai, Los Angeles, CA, USA. ²Karsh Division of Gastroenterology and Hepatology, Department of Medicine, Cedars-Sinai, Los Angeles, CA, USA. ³Division of Endocrinology, Diabetes, and Metabolism, Department of Medicine, Cedars-Sinai, Los Angeles, CA, USA. ✉email: mark.pimentel@cshs.org

breath test, and another with elevated hydrogen sulfide (H₂S) on breath test and elevated H₂S-producing bacteria such as genus *Fusobacterium* and *Desulfovibrio* spp.⁸

Further, a separate human study combining culture and next generation sequencing has revealed that 2 strains of *Escherichia coli* and 2 species of *Klebsiella* dominate the small bowel microbiome in SIBO⁹. In fact, these few strains and species, all of which are members of the H₂-producing family Enterobacteriaceae, together account for 40.24% of all duodenal bacteria in SIBO subjects, as compared to 5.6% in non-SIBO subjects⁹. Of these, an *E. coli* strain with genomic similarities to strain K-12 correlated with a wide variety of GI symptoms, including bloating, abdominal pain, diarrhea, and urgency⁹. Importantly, these microbes typically colonize the mucus layer in the small bowel¹⁰, and by doing so, may partially isolate themselves from the effects of the hydrophobic, non-absorbable rifaximin.

One possible mechanism underlying the development of SIBO in IBS-D is a previous episode of acute gastroenteritis, formerly known as post-infection IBS¹¹. The pathogen most strongly implicated in IBS-D is *Campylobacter jejuni*¹². Animal models of exposure to *C. jejuni* strongly support a causal role for *C. jejuni* in the development of IBS-D^{13–15}, and further demonstrate that this may be due specifically to the bacterial toxin cytolethal distending toxin B (CdtB), which exhibits molecular mimicry to the host protein vinculin, leading to the development of autoimmunity^{14,16}. Significantly, it has been shown that inoculating rats with the CdtB toxin alone results in IBS-D-like phenotypes including increased stool wet weight (a diarrhea-like phenotype) and SIBO^{17,18}. Most recently, the SIBO in CdtB-inoculated rats was shown to comprise distinct microtypes, including one with overgrowth of the hydrogen producer *E. coli*, and another with overgrowth of hydrogen sulfide producer *Desulfovibrio*¹⁸, echoing findings in human subjects^{8,9}. Moreover, these microbial changes were associated with distinct changes in host intestinal gene expression profiles, including changes associated with alterations in gut permeability, visceral hypersensitivity, and alterations in gut motility¹⁸, validating this model as an accurate reproduction of human IBS-D.

Given the limited effectiveness of rifaximin in human IBS patients (only 44%), and knowing that key genera in SIBO such as *Escherichia* and *Klebsiella* can find safe harbor in the mucus layer of the small intestine¹⁰, the goal of this study is to assess whether adding a mucolytic (*N*-acetylcysteine [NAC]) to rifaximin more completely eradicates SIBO in an animal model of IBS-D. To do this, we first determine the optimal combination of rifaximin and NAC, and then conduct a randomized controlled trial to compare the efficacy of this combination of rifaximin plus NAC to rifaximin alone in treating phenotypes in the validated rat model of IBS-D generated via CdtB inoculation¹⁸.

Methods

Identifying the optimal combination of rifaximin and NAC

A resazurin checkerboard method¹⁹ was used to evaluate the effects of different combinations of rifaximin and NAC on an *E. coli* clinical isolate. This organism was chosen as *E. coli* overgrowth was recently found to be one of the dominant small bowel microtypes in a validated IBS-D rat model generated by inoculating rats with CdtB¹⁸, and *E. coli* is also one of the dominant organisms in human subjects with SIBO⁹. Microtiter plates were prepared by serially diluting rifaximin along the x-axis and NAC along the y-axis. A fresh *E. coli* suspension was dispensed into each well for a final concentration 5×10^5 CFU/mL, after which 30 μ l of resazurin solution was added to each well. The plates were covered and incubated at 37 °C overnight (18–24 h). A change from blue to pink indicated reduction of resazurin to resorufin, reflecting bacterial growth/viability. Experiments were performed in triplicate.

To evaluate whether the combined effects of rifaximin and NAC are synergistic, antagonistic, or indifferent, the fractional inhibitory concentration index (FICI) was calculated using the minimum inhibitory concentration (MIC) of each compound as follows: $FICI = (A/MICA + B/MICB)$ where A and B are the MIC of each compound in combination (in a single well), and MICA and MICB are the MIC of each drug individually. The results were interpreted by the FICI as: synergism, < 0.50; indifference, 0.50–4; and antagonism, > 4.

Animal model and study overview

The generation of the CdtB-inoculated rats used in this study has been detailed in a separate publication¹⁸. Briefly, a total of 226 male 12-week old Sprague–Dawley rats, obtained from Envigo, Somerset, NJ, were included in this study. Rats were housed under regular 12/12 h light–dark cycles with ad libitum access to food and water. The study protocol including all experimental protocols was approved by the Cedars-Sinai Institutional Animal Care and Use Committee (IACUC #8107). All methods and protocols were carried out in accordance with all relevant guidelines and regulations, and all methods are reported in accordance with the ARRIVE guidelines.

Baseline measurements were obtained for the entire rat cohort, including levels of serum cytokines and anti-CdtB antibodies, as well as three-day stool consistency assessments¹⁸. Upon completion of the baseline assessments, the rats were randomized into 2 different groups. One group was inoculated with recombinant *C. jejuni* CdtB protein (CdtB group, N = 178) (Fig. 1)¹⁸, and the second group was injected with vehicle alone (controls, N = 48) (Fig. 1)¹⁸. Subcutaneous injections were performed as described previously¹⁷, with all rats receiving an initial inoculation followed by a booster inoculation 3 weeks later, per our established and validated protocol^{17,18}. For the CdtB group, each animal initially received a total of 90 μ g CdtB, given as 5×100 μ l injections (each containing 18 μ g CdtB) at distinct sites on the animal's back, followed 3 weeks later by booster injections containing a total of 54 μ g CdtB, given as 3×100 μ l injections^{17,18}. Control animals were injected in the same manner, but with vehicle alone^{17,18}. After completion of the initial and booster injections, measurements of serum cytokines and anti-CdtB antibody levels as well as stool consistency were repeated, to determine the effects of CdtB on these parameters¹⁸.

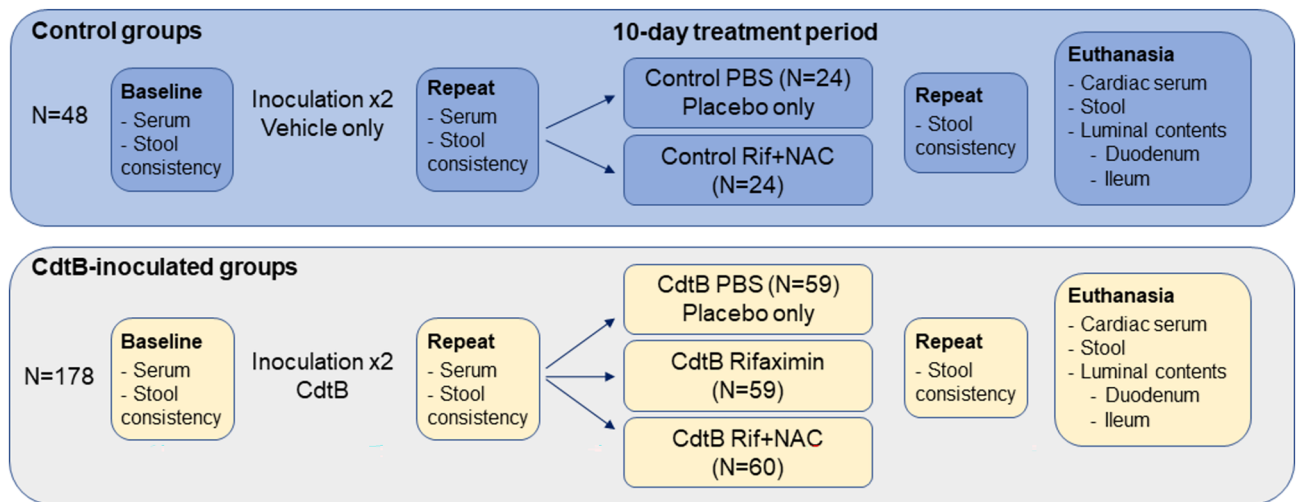


Figure 1. Study Design. After baseline collections, rats received 2 inoculations, 3 weeks apart, of vehicle only (control groups) or CdtB (CdtB-inoculated groups). Following repeat evaluations 7 weeks after the last inoculation, the rat groups were further subdivided and treated with placebo (PBS), rifaximin alone, or rifaximin plus NAC, for 10 days. NAC = N-acetylcysteine.

For the present study, the rats were then subdivided into 5 different groups—2 groups of control rats and 3 groups of CdtB-inoculated (CdtB) rats—for treatment with placebo, rifaximin alone, or the optimal combination of rifaximin and NAC identified in the resazurin checkerboard assay. Half of the control group (N = 24) was gavaged with placebo (1 ml of 1 × PBS) daily for 10 days (Control PBS group), and the other half (N = 24) was gavaged with 1 ml of 1 × PBS containing 1.65 mg rifaximin and 14 mg NAC daily for 10 days (Control Rif + NAC, safety group). The safety group was included to assess the effects of combined rifaximin and NAC treatment on the normal rat gut microbiome.

For CdtB-inoculated rats, the first group (N = 59) was gavaged with placebo (1 ml of 1 × PBS) daily for 10 days (CdtB PBS group), the second group (N = 59) was gavaged with 1 ml of 1 × PBS containing 1.65 mg rifaximin alone daily for 10 days (CdtB Rifaximin group), and the third group (N = 60) was gavaged with 1 ml of 1 × PBS containing 1.65 mg rifaximin and 14 mg NAC daily for 10 days (CdtB Rif + NAC).

After completion of the 10-day treatment period, stool consistency was reassessed in all rats. The rats were then euthanized via CO₂ asphyxiation followed by pneumothorax. On the day of euthanasia, cardiac serum was collected, and luminal contents from the duodenum, ileum, and colon were harvested for microbial analysis as detailed below.

Serum and stool collection

Blood and stool samples were collected from each rat at baseline, 7 weeks after the booster injections, and after completion of the 10-day treatment period prior to euthanasia (Fig. 1), using the techniques described previously¹⁸. Blood was collected from tail vein into sterile 2.0 mL tubes, allowed to coagulate for at least 30 min, and then centrifuged. Serum aliquots were prepared and stored at -80 °C. At euthanasia, cardiac blood was collected, and serum was obtained and prepared as for the tail vein bleeds.

Stool samples collected prior to euthanasia were obtained via stimulation of the anus under manual restraint in order to guarantee fresh stool, and stool consistency was determined as described previously¹⁸. At euthanasia, stool samples were collected directly from the colon.

Small bowel content collection at euthanasia

At euthanasia, luminal contents from segments of the small intestine (duodenum and ileum) were collected and stored at -80 °C prior to DNA isolation. Small bowel segments included the duodenum (a segment 5 cm distal to the pylorus) and the ileum (a segment 5 cm proximal to the ileocecal valve).

Determination of serum cytokine levels

The inflammatory profiles of all rats were determined in serum collected after the booster injections and at euthanasia. Circulating cytokine and chemokine levels were analyzed using a bead-based multiplex panel comprising interleukin (IL) 4, IL1β, IL2, IL6, IL13, IL10, IL12p70, IL5, IL18, interferon gamma (IFNγ), monocyte chemoattractant protein-1 (MCP1), and tumor necrosis factor alpha (TNFα) (EDM Millipore, Billerica, MA), on a Luminex FlexMap 3D (Luminex Corporation, Austin, TX).

The fold change differences between groups and *P*-values (< 0.05) for each cytokine and chemokine were uploaded to Ingenuity Pathway Analysis (IPA, Summer Release 2022) software to identify altered pathways after CdtB exposure followed by the different treatments. The fold changes (protein expression levels) were used to perform a Core Analysis for the identification of canonical pathways and their possible top upstream regulators.

DNA extraction from small bowel luminal samples and stool

Small bowel and stool samples were thawed on ice and weighed. The MagAttract PowerMicrobiome DNA/RNA EP Kit (Qiagen) was used to isolate microbial DNAs. DNAs were purified using a KingFisher Duo automated system (ThermoFisher), and quantified using the NanoDrop One fluorometer (ThermoFisher) and with the Qubit DNA Broad Range Assay kit (Invitrogen, Carlsbad, CA) on a Qubit 4 Fluorometer (Invitrogen).

Bacterial total load analysis

Total bacterial loads were assessed by measuring the number of 16S gene copies in each small bowel and stool sample using the Pan Bacterial 1 assay (Qiagen) as described previously¹⁸. Total DNA extracted from 1 mL of a bacterial culture containing 9×10^8 colony forming units (CFU) (approximately 15 ng) was used to create a standard curve, and the final concentration of 16S rRNA gene copies in each sample was determined by comparing the resulting Ct of each sample against the standard curve, correcting for dilutions and normalizing to the extracted sample weight as described previously¹⁸.

Escherichia coli and *Desulfovibrio* spp. load analysis

Bacterial loads for *E. coli* were assessed by measuring the number of 16S gene copies in each sample using an *Escherichia* spp. assay (Qiagen) as described previously¹⁸, and bacterial loads for *Desulfovibrio* spp. were assessed by developed primers by Fite et al.²⁰ and custom produced by Eurofins Scientific.

Desulfovibrio spp. measurements were carried out on a Bio-Rad CFX96 Real-Time PCR Detection System using: 10 μ L of Power SYBR Green PCR Master Mix (Applied Biosystems), 4 μ L of each primer at 3 μ M, and 2 μ L of genomic DNA, for a final volume of 20 μ L. Thermocycling conditions were: 95 °C for 10 min, then 40 cycles of 95 °C for 15 s, 60 °C for 1 min.

Quantitation was determined creating a standard curve using extracted DNA from *D. desulfuricans* ATCC 27,774 (measured at 34.3 ng/ μ L). Serial dilutions were prepared and analyzed and the final concentration of 16S rRNA gene copies was determined as described above.

Statistical analysis

Paired and group analyses were performed using GraphPad Prism 9.1.0 (GraphPad Software) and IBM SPSS Statistics Version 24. Normally distributed data were analyzed by t-test or paired t-test, and data that were not normally distributed were analyzed by Mann–Whitney test or Wilcoxon paired test. Correlations were performed using Spearman's rank correlations.

Results

Optimal concentrations of rifaximin and NAC for inhibition of *E. coli*

Based on the resazurin checkerboard assay (Fig. 2), the minimum inhibitory concentration (MIC) for rifaximin alone, revealed by row H2 to H12 (Fig. 2), was 8 μ g/mL (well H7). The MIC for NAC alone, revealed by wells A1 to G1, was 4 ng/mL (well B1). The resulting MIC for the combination of both drugs was 4 μ g/mL (rifaximin) and 0.125 ng/mL (NAC) (well G8). Considering the resulting fractional inhibitory concentration index (FICI) of 0.503, NAC at a concentration of 0.125 ng/mL had no antagonistic effect on rifaximin activity. Moreover, there is a potential synergistic effect of NAC on rifaximin, as the rifaximin MIC improved by 50% (8 μ g/mL to 4 μ g/mL) when combined with NAC. Even at higher concentrations, NAC had no antagonistic effects on rifaximin (wells E7 and F7). Based on the checkerboard assay and adjusting doses for rat body weights, it was determined that the optimal daily doses for administration in rats were 1.65 mg of rifaximin and 14 mg of NAC.

Development of antibodies to CdtB and IBS-D-like phenotypes

Consistent with our previous findings for this model¹⁷, inoculation of rats with CdtB resulted in an increase in anti-CdtB antibodies (OD 3.07 ± 0.82) compared to control rats which were not inoculated with CdtB (OD 0.06 ± 0.04 , $P < 0.0001$)¹⁸. Rats inoculated with CdtB also had higher stool wet weights (63.2 ± 3.2) when compared to control rats (61.4 ± 3.5 , $P = 0.0002$), and the levels of anti-CdtB correlated with stool wet weights ($R = 0.443$, $P = 0.001$)¹⁸.

Treatment with rifaximin plus NAC reduced stool consistency variance in CdtB-inoculated rats

Stool consistency was determined in all rats. Consistent with our previous findings for this model¹⁷, CdtB-inoculated rats had higher wet weights when compared to controls¹⁸. Further analysis following completion of treatments revealed that control rats exhibited a low day-to-day variance in stool consistency ($P = 0.35$), as well as low variability within the group on a given day (Control PBS group, Fig. 3a), whereas CdtB-inoculated rats treated with placebo exhibited a wide day-to-day variance in consistency ($P = 0.0014$), as well as greater variability in stool consistency within the group each day (CdtB PBS group, Fig. 3b). This did not improve in CdtB-inoculated rats that were treated with rifaximin alone (CdtB Rifaximin group) (Fig. 3c). However, the variance in stool consistency, and the variability in stool consistency within the group, were normalized in CdtB-inoculated rats treated with rifaximin plus NAC (CdtB Rif + NAC group) (Fig. 3d).

Small bowel *E. coli* and *Desulfovibrio* levels

CdtB-inoculated rats developed higher small bowel *E. coli* levels, as determined by qPCR, when compared to control rats ($P = 0.05$, Fig. 4A). Treatment with rifaximin alone (CdtB Rifaximin group) was not sufficient to normalize *E. coli* levels when compared to CdtB-inoculated rats treated with placebo (CdtB PBS group) ($P = 0.96$, Fig. 4A). However, CdtB-inoculated rats that were treated with rifaximin plus NAC (CdtB Rif + NAC group)

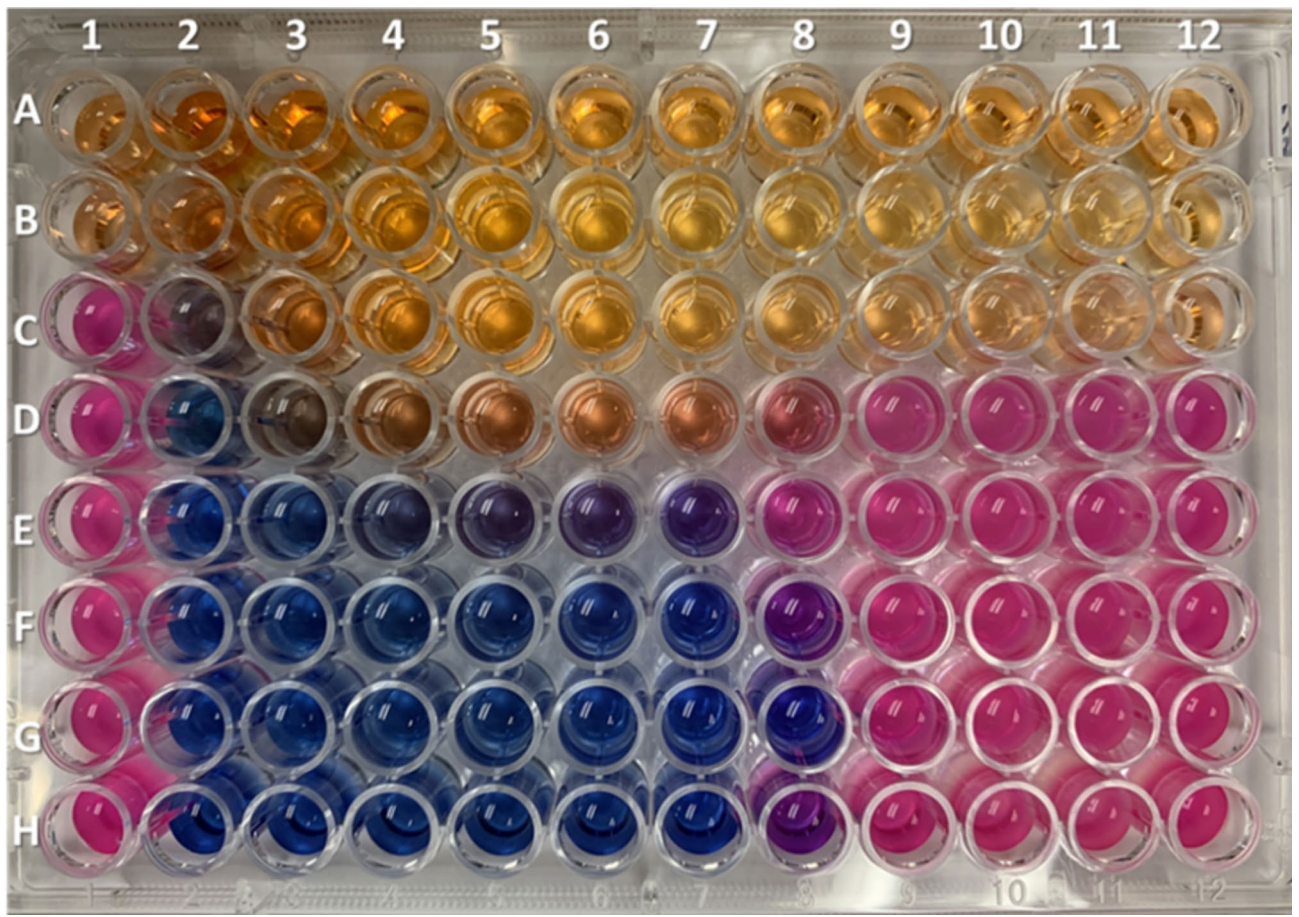


Figure 2. Checkerboard assay to evaluate the effects of combining rifaximin and NAC on *Escherichia coli*. Wells A1 to G1 represent the MIC of NAC alone (8 mg/mL to 0.125 mg/mL). H1 is a positive control for growth. Wells A2 to G2 through A12 to H12 represent the MIC of NAC and rifaximin combined at different concentrations for both drugs. Wells H2 to H12 represent the MIC for rifaximin alone (256 µg/mL to 0.25 µg/mL). Blue color: no bacterial growth. Pink color: bacterial growth.

exhibited *E. coli* levels that were comparable to control rats ($P=0.26$), and significantly lower than in placebo-treated CdtB-inoculated rats (CdtB PBS group) ($P=0.0021$, Fig. 4A).

Small bowel *Desulfovibrio* spp. DNA levels were also determined by qPCR. CdtB-inoculated rats (CdtB PBS group) had higher levels of species from this genus when compared to controls ($P=0.0012$, Fig. 4B). However, CdtB-inoculated rats that were treated with rifaximin plus NAC (CdtB Rif + NAC group) exhibited *Desulfovibrio* spp. levels that were comparable to those in controls ($P=0.06$) and significantly lower than in placebo-treated CdtB-inoculated rats (CdtB PBS group) ($P=0.013$, Fig. 4B).

In addition, total bacterial loads decreased in the duodenum of CdtB-inoculated rats treated with rifaximin plus NAC (CdtB Rif + NAC group) when compared to CdtB-inoculated rats treated with placebo (CdtB PBS group) ($P=0.02$) or with rifaximin alone (CdtB Rifaximin group) ($P=0.0005$, Fig. 5). No changes were seen in the ileum.

Inflammatory mediators and response to antibiotics

Inflammatory markers change in response to CdtB inoculation in a manner that appears dependent on the development of microbiome changes in the gut, as previously described for this model¹⁷. Examining the inflammatory markers in all groups, it is clear that cytokine levels in the CdtB Rif + NAC group normalized to control levels following treatment (Table 1, Fig. 6). Further, based on IPA analysis, the change in cytokines following treatment in the CdtB Rif + NAC group predicted that there would be an improvement in diarrhea, driven specifically by a reduction in peptidoglycan and *E. coli* levels (Fig. 6), consistent with our stool consistency findings in this group.

Discussion

In this study, using a combination of rifaximin and the mucolytic NAC was superior to rifaximin alone in improving stool consistency and variability, changes in microbial populations, and cytokine levels in a validated rat model of IBS-D. Most notably, levels of *Desulfovibrio* spp. and *E. coli*, both of which are elevated in human subjects^{8,9}, were also elevated in the small bowel of CdtB-inoculated rats, but were normalized in rats treated with rifaximin plus NAC. Total bacterial levels in the small bowel were also elevated in CdtB-inoculated rats,

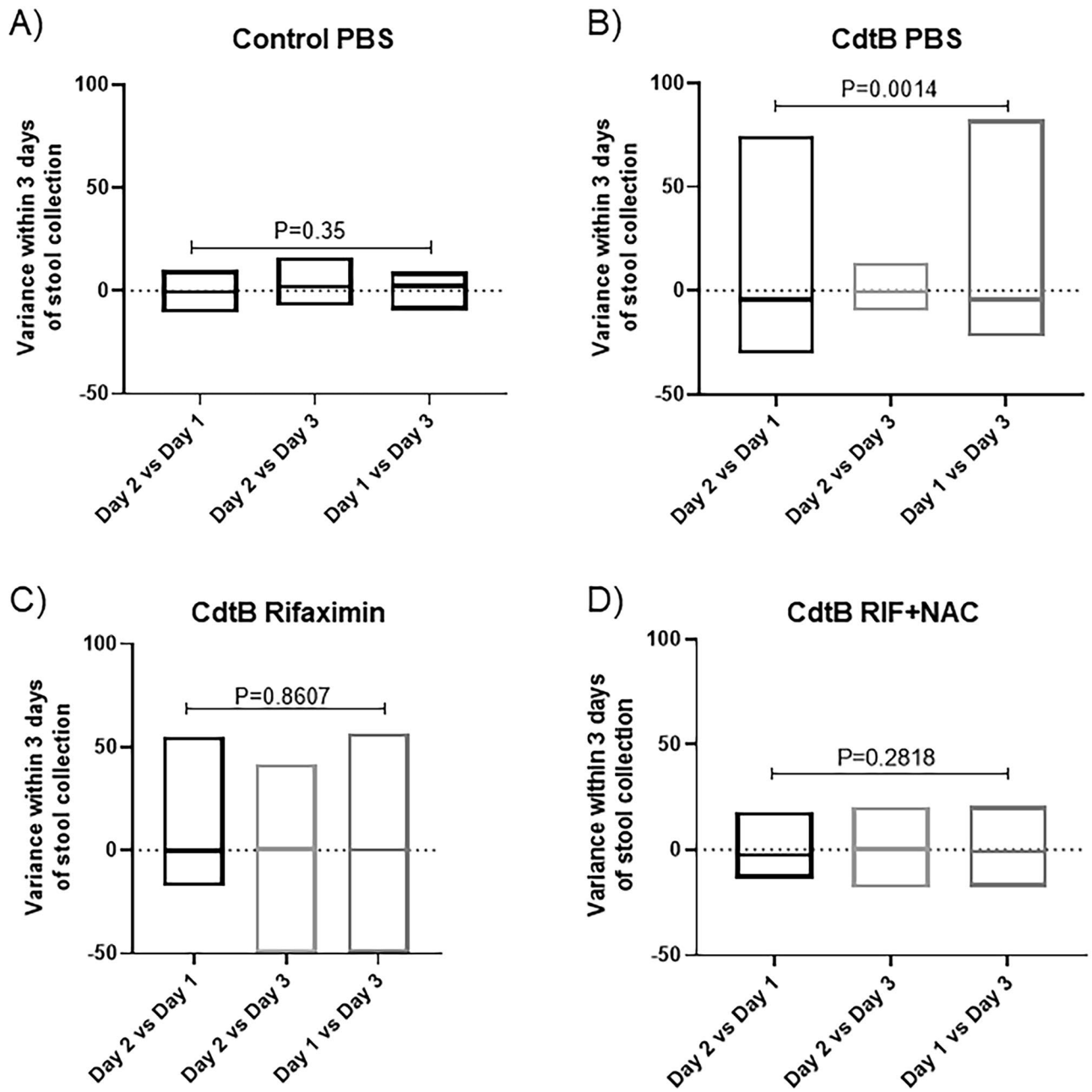


Figure 3. Stool consistency variance in controls (A) and in CdtB-inoculated rats treated with vehicle (B), rifaximin alone (C), or rifaximin plus NAC (D) after completion of the 10-day treatment periods. Data are presented as boxplots (min to max).

but were reduced to levels not different from controls in CdtB-inoculated rats treated with rifaximin plus NAC. Importantly, treatment with the combination of rifaximin and NAC did not have any effects on *E. coli* or *Desulfovibrio* spp. levels or total bacterial loads in placebo-inoculated control rats.

This study marks the convergence of several key concepts and lines of study in IBS. In the past, IBS was principally diagnosed based on a constellation of symptoms in the absence of red flags and other conditions^{21,22}. However, more recently, evidence is accumulating that in a large percentage of patients, IBS has an organic basis. One of the most well-studied mechanisms for the development of IBS is that IBS can be triggered by acute gastroenteritis, and a landmark meta-analysis suggests that after acute gastroenteritis, 11% of subjects subsequently develop new onset IBS²³. The strongest evidence for this is for the pathogen *Campylobacter jejuni*¹², through molecular mimicry between the bacterial pathogen CdtB and the host cytoskeletal protein vinculin^{14,16}. Another consistent finding in IBS is alterations in the gut microbiome^{1,24}. The most consistent microbiome finding in IBS-D is small intestinal bacterial overgrowth (SIBO), which is diagnosed via a positive H₂ breath test^{5,6}, and a recent meta-analysis concluded that breath testing and small bowel culture studies support that a significant proportion of IBS subjects suffer from SIBO⁴. Extending these findings, a recent study for the first time combining breath testing, gastrointestinal symptoms, and microbiome analysis, found that IBS-D is associated with

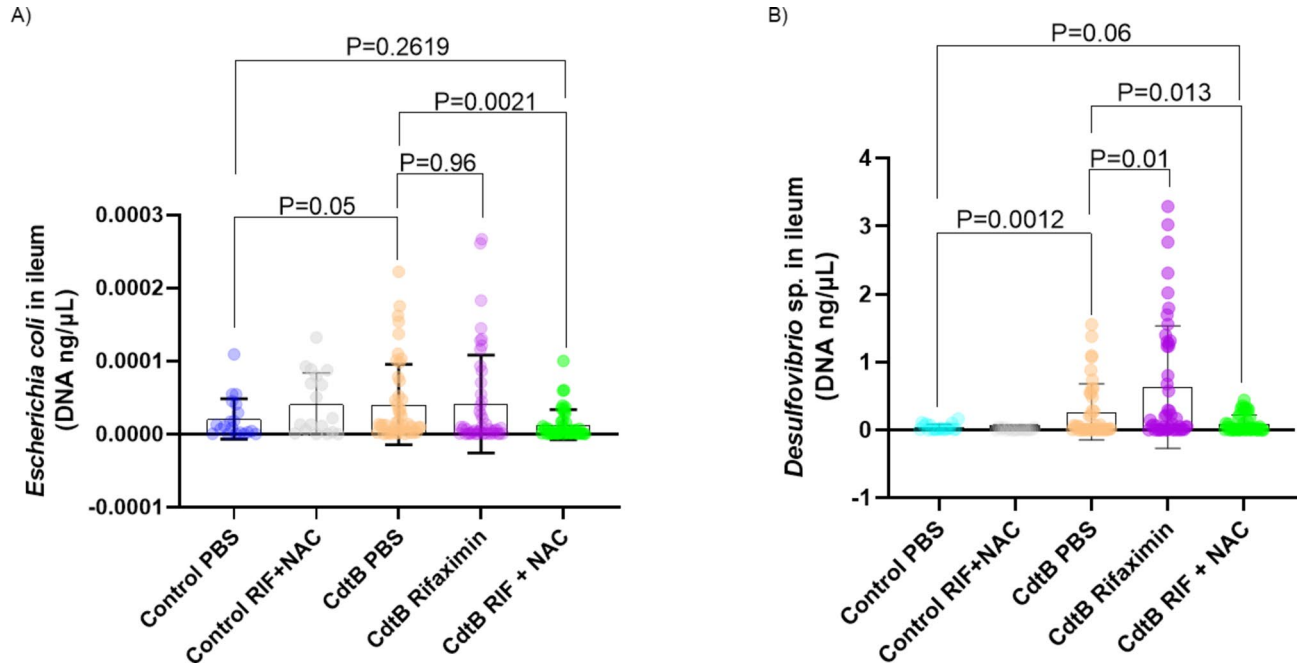


Figure 4. (A) *Escherichia coli* DNA levels in the small bowel in all groups after treatment. (B) *Desulfovibrio* spp. DNA levels in the small bowel in all groups after treatment. Data are presented as mean ± standard deviation.

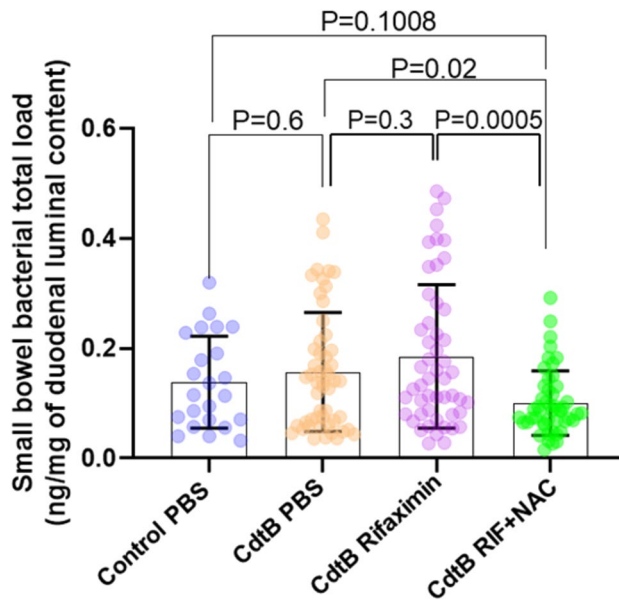


Figure 5. Levels of total bacteria in the small bowel in all groups after treatment. Data are presented as mean ± standard deviation.

two gut microtypes, one associated with increased H₂ on breath test, and another associated with increased H₂S on breath test coupled with increased H₂S-producing bacteria such as *Fusobacterium* and *Desulfovibrio* spp⁸. That these H₂S-producing gut microbes contribute to the development of an IBS-D microtype was further supported by a recent animal study in which gavaging rats with *Fusobacterium* or *Desulfovibrio* species, specifically *F. varium* or *D. piger*, resulted in IBS-D-like phenotypes including diarrhea-like stool consistency and gut microbiome alterations²⁵. Another recent study combining high-throughput sequencing with small bowel culture and gastrointestinal symptoms in human subjects with SIBO showed that very few specific *E. coli* and *Klebsiella* strains/species appear to dominate the microbiome in SIBO, and correlate with the severities of abdominal pain, diarrhea, and bloating in these subjects⁹.

	Control: PBS		Control: Rif+NAC		CdtB: PBS		CdtB: Rif		CdtB: Rif+NAC	
	Mean (pg/mL)	SD	Mean (pg/mL)	SD	Mean (pg/mL)	SD	Mean (pg/mL)	SD	Mean (pg/mL)	SD
IL18	420.52	191.50	349.61	199.46	496.05	239.65	362.07	240.58	401.13	228.05
IL1β	56.46	30.02	48.41	33.89	67.31	38.39	47.09	37.51	52.44	36.41
TNFα	11.05	4.24	9.96	4.83	12.56	5.15	9.49	5.18	10.36	4.89
IL2	300.74	137.60	255.16	146.43	352.45	173.37	255.83	168.06	273.20	151.29
IL4	359.36	146.64	304.91	173.88	394.57	176.92	298.14	196.61	326.60	175.56
IL6	3811.09	2492.67	2962.63	2545.17	4237.16	3096.76	2940.03	2869.32	3059.31	2432.18
IL13	66.29	26.02	58.19	30.28	73.14	33.39	58.42	34.72	61.17	29.55
IL10	117.11	61.88	88.16	64.97	128.00	80.63	90.35	77.06	99.60	71.27
IL12p70	780.83	377.78	692.63	396.58	913.06	413.13	649.24	406.08	694.85	383.76
IFN γ	827.00	400.30	662.77	436.34	888.91	473.25	640.63	501.87	701.11	449.84
IL5	288.20	83.12	262.12	100.26	307.41	96.91	252.08	103.16	272.47	98.63
MCP1	860.74	214.17	797.11	236.13	933.91	257.85	774.64	260.86	811.78	244.23

Table 1. Serum levels of pro- and anti-inflammatory cytokines post-treatment in controls and CdtB-inoculated (CdtB) rats. Pro-inflammatory cytokines altered in response to combined treatment with rifaximin plus NAC in CdtB-inoculated rats as compared to controls (shown in Fig. 6) are indicated in bold.

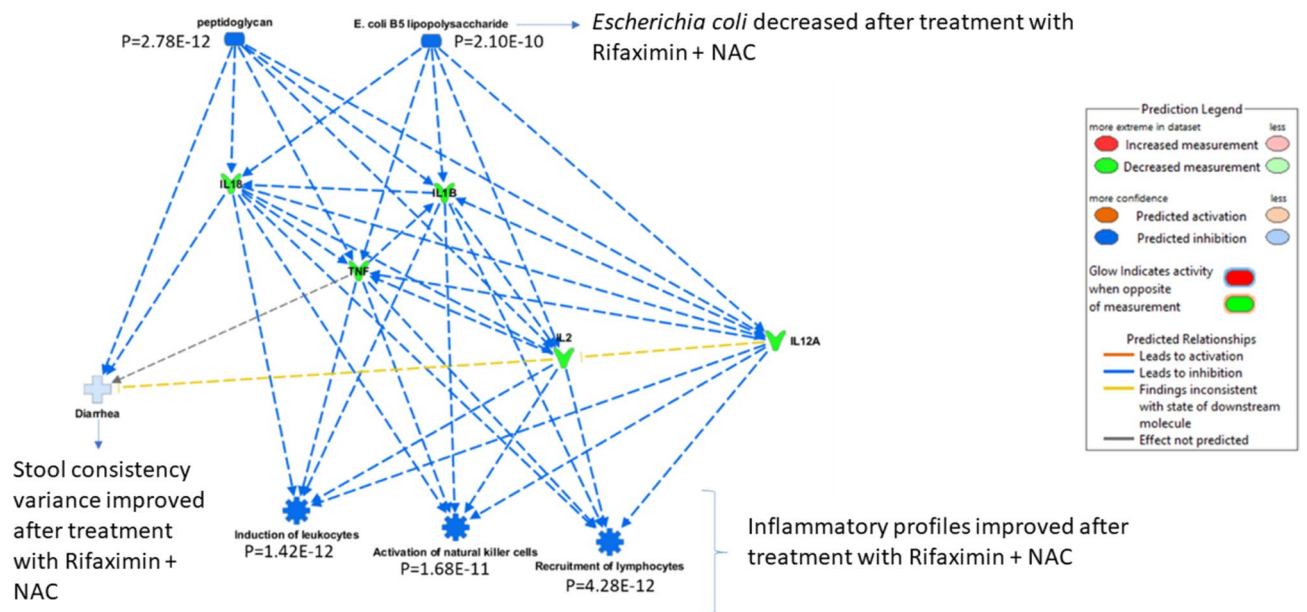


Figure 6. IPA analysis of change in cytokines in response to combined treatment with rifaximin plus NAC in CdtB-inoculated rats as compared to controls.

A final link in this convergence of microbiome-based data and mechanisms in IBS is a recent study demonstrating that direct inoculation of rats with the CdtB toxin, which we previously showed results in IBS-D-like phenotypes in rats¹⁷, also results in the development of distinct gut microtypes, one of which was dominated by increased prevalence of *Escherichia-Shigella* and higher absolute abundance of *E. coli*, and another that was dominated by increased prevalence of *Desulfovibrio*¹⁸. Significantly, transcriptomics analysis in ileal tissues from these rats revealed alterations in host microRNA-mRNA interactions controlling intestinal permeability, visceral hypersensitivity/pain, and gastrointestinal motility genes, including several previously associated with IBS¹⁸. Taken together, these studies suggest that IBS-D can be triggered by the CdtB toxin, resulting in gut microbiome alterations that can be parsed into at least 2 microtypes, one associated with increased H₂S producers such as *Desulfovibrio*, and one associated with increased H₂-producers such as *E. coli*, and which alter host transcriptomics associated with intestinal permeability, visceral hypersensitivity, and gastrointestinal motility.

Some of the earliest evidence that at least a proportion of IBS-D patients have microbiome changes linked to the pathophysiology of the condition came from the fact that IBS-D could be treated with antibiotics, particularly rifaximin (a non-absorbed antibiotic)^{2,3}, which was subsequently approved by the FDA for the treatment of IBS-D²⁶. Data from the pivotal final study for approval suggested that treating IBS-D with rifaximin 550 mg three times daily for 14 days resulted in 44% of IBS-D subjects achieving the primary endpoint of improvement

in abdominal pain and diarrhea³. Interestingly, this response rate was dependent on a positive breath test for SIBO²⁷. However, it remained unclear why the response rate was only 44%.

As noted above, analysis of the small bowel microbiome has shown that *E. coli* and *Klebsiella* are key disruptors of the normal microbiome in SIBO⁹. Importantly, Enterobacteriaceae family members, including *E. coli* and *Klebsiella*, are facultative anaerobes and colonize the viscous mucus of the small bowel¹⁰. As a result, a comprehensive examination of the small intestinal microbiome requires mucolysis of samples to assess the total composition¹⁰. Since rifaximin is a hydrophobic molecule, which is part of the reason for its low intestinal absorption, it is unlikely to penetrate intestinal mucus, and thus *E. coli* and *Klebsiella* in this microenvironment could be protected from the effects of rifaximin.

In this study, we hypothesized that rifaximin could be better optimized based on an understanding of the potential roles of these microenvironments in the dysbiosis in IBS-D. Specifically, we hypothesized that adding a mucolytic, such as NAC, to rifaximin could improve its ability to treat IBS-D. The results of the resazurin assay indicate that not only did NAC improve the ability of rifaximin to eliminate *E. coli* in vitro, it unexpectedly did so at a much lower dose than is clinically prescribed. When this combination of low dose rifaximin and NAC was tested in a validated animal model of CdtB-induced IBS-D, rats treated with rifaximin plus NAC exhibited reduced levels of total bacteria in the small bowel, as well as specific reductions in both *E. coli* and *Desulfovibrio* levels. These rats also exhibited normalized variance in stool consistency. With the exception of the reduction in *Desulfovibrio* levels, these changes were not seen in rats treated with rifaximin only.

There were also changes in cytokine levels seen in this study. Specifically, rats treated with rifaximin plus NAC exhibited normalized cytokine profiles that approximated those in the control group. This was not as evident in rats treated with rifaximin alone. In fact, IPA analysis predicted that these changes in cytokine profiles following treatment with rifaximin plus NAC would be associated with a reduction in peptidoglycan, reduction in *E. coli* levels, and an improvement in diarrhea. Thus, rifaximin with NAC is superior to rifaximin alone in the treatment of this rat model of IBS-D.

There are some limitations to this study. This is of course an animal study. It would be important to assess whether the use of a combination of rifaximin and NAC in humans with IBS-D would have a greater benefit than rifaximin alone. It would also be interesting to assess the effects of combined treatment with rifaximin plus NAC on the microbiome as a whole, which would be best done at least a month after the completion of treatment. In addition, NAC itself has previously been shown to have independent antimicrobial properties²⁸, albeit at significantly higher concentrations than those used in this study (80 mg/ml vs. 0.125 ng/mL). Our resazurin checkerboard assay indicated a MIC for NAC alone of 4 ng/mL. Nonetheless, it is possible that the low concentrations of NAC used here may have had slight antimicrobial effects in addition to the mucolytic effects. Lastly, while small intestinal microbiome profiles in rats are similar to humans, an exception is that rats do not generally have significant levels of *Klebsiella* in their microbiome, so it was not possible to assess the effects of combined treatment with rifaximin plus NAC on *Klebsiella* here.

In conclusion, based on the importance of mucus in the small bowel in the microbiome changes in IBS-D, the optimal combination of rifaximin and the mucolytic *N*-acetylcysteine (NAC) tested here resulted in a normalization of the microbiome compared to rifaximin alone. This combination of rifaximin plus NAC also resulted in a greater normalization of bowel function and cytokine profiles. It is clear that failure to affect microbes in the small bowel mucus could be what is mitigating a greater benefit of rifaximin in human clinical trials. All data now indicate that there are two microtypes in IBS-D, one associated with H₂ on breath test and SIBO with overgrowth of *E. coli*, and another associated with H₂S on breath test, which only because detectable recently⁸, and overgrowth of *Fusobacterium* and *Desulfovibrio*. This novel combination of rifaximin plus NAC appear to be effective against both of these microtypes. This greater understanding of the small bowel microbiome in IBS will be used to help improve the treatment of IBS-D patients.

Data availability

The authors confirm that the data supporting the findings of this study are available within the manuscript.

Received: 31 May 2024; Accepted: 1 August 2024

Published online: 05 August 2024

References

- Pimentel, M. & Lembo, A. Microbiome and its role in irritable bowel syndrome. *Dig. Dis. Sci.* **65**, 829–839 (2020).
- Pimentel, M. *et al.* Rifaximin therapy for patients with irritable bowel syndrome without constipation. *N Engl J Med* **364**, 22–32 (2011).
- Lembo, A. *et al.* Repeat treatment with rifaximin is safe and effective in patients with diarrhea-predominant irritable bowel syndrome. *Gastroenterology* **151**, 1113–1121 (2016).
- Shah, A. *et al.* Small intestinal bacterial overgrowth in irritable bowel syndrome: A systematic review and meta-analysis of case-control studies. *Am J Gastroenterol* **115**, 190–201 (2020).
- Rezaie, A. *et al.* Hydrogen and methane-based breath testing in gastrointestinal disorders: The North American Consensus. *Am J Gastroenterol* **112**, 775–784 (2017).
- Pimentel, M. *et al.* ACG clinical guideline: Small intestinal bacterial overgrowth. *Am. J. Gastroenterol.* **115**, 165–178 (2020).
- Ghoshal UC, Sachdeva S, Ghoshal U, *et al.* Asian-Pacific consensus on small intestinal bacterial overgrowth in gastrointestinal disorders: An initiative of the Indian neurogastroenterology and motility association. *Indian J. Gastroenterol* 2022.
- Villanueva-Millan MJ, Leite G, Wang J, *et al.* Methanogens and Hydrogen Sulfide Producing Bacteria Guide Distinct Gut Microbe Profiles and Irritable Bowel Syndrome Subtypes. *Am J Gastroenterol* 2022.
- Leite G, Rezaie A, Mathur R, *et al.* Defining small intestinal bacterial overgrowth by culture and high throughput sequencing. *Clin. Gastroenterol. Hepatol.* 2023.
- Leite, G. G. S. *et al.* Optimizing microbiome sequencing for small intestinal aspirates: Validation of novel techniques through the REIMAGINE study. *BMC Microbiol.* **19**, 239 (2019).

11. Thabane, M. & Marshall, J. K. Post-infectious irritable bowel syndrome. *World J. Gastroenterol. WJG* **15**, 3591–3596 (2009).
12. Takakura W, Kudaravalli P, Chatterjee C, et al. Campylobacter infection and the link with Irritable Bowel Syndrome: On the pathway towards a causal association. *Pathog Dis* 2022;80.
13. Pimentel, M. *et al.* A new rat model links two contemporary theories in irritable bowel syndrome. *Dig Dis Sci* **53**, 982–989 (2008).
14. Pokkunuri, V. *et al.* Role of cytolethal distending toxin in altered stool form and bowel phenotypes in a rat model of post-infectious irritable bowel syndrome. *J Neurogastroenterol. Motil.* **18**, 434–442 (2012).
15. Pimentel, M. *et al.* Autoimmunity links vinculin to the pathophysiology of chronic functional bowel changes following campylobacter jejuni infection in a rat model. *Dig. Dis. Sci.* **60**, 1195–1205 (2015).
16. Sung, J. *et al.* Effect of repeated campylobacter jejuni infection on gut flora and mucosal defense in a rat model of post infectious functional and microbial bowel changes. *Neurogastroenterol. Motil.* **25**, 529–537 (2013).
17. Morales W, Triantafyllou K, Parodi G, et al. Immunization with cytolethal distending toxin B produces autoantibodies to vinculin and small bowel bacterial changes in a rat model of postinfectious irritable bowel syndrome. *Neurogastroenterol. Motil.* 2020:e13875.
18. Leite, G. *et al.* Cytolethal distending toxin B inoculation leads to distinct gut microtypes and IBS-D-like microRNA-mediated gene expression changes in a rodent model. *Gut. Microbes* **16**, 2293170 (2024).
19. Palomino, J. C. *et al.* Resazurin microtiter assay plate: Simple and inexpensive method for detection of drug resistance in *Mycobacterium tuberculosis*. *Antimicrob. Agents Chemother.* **46**, 2720–2722 (2002).
20. Fite, A. *et al.* Identification and quantitation of mucosal and faecal desulfovibrios using real time polymerase chain reaction. *Gut* **53**, 523–529 (2004).
21. Drossman, D. A. The functional gastrointestinal disorders and the Rome III process. *Gastroenterology* **130**, 1377–1390 (2006).
22. Lacy, B. E., & Patel, N. K. Rome criteria and a diagnostic approach to irritable bowel syndrome. *J. Clin. Med. Res.* 2017;6.
23. Klem, F. *et al.* Prevalence, risk factors, and outcomes of irritable bowel syndrome after infectious enteritis: A systematic review and meta-analysis. *Gastroenterology* **152**, 1042–1054.e1 (2017).
24. Singh, P. & Lembo, A. Emerging role of the gut microbiome in irritable bowel syndrome. *Gastroenterol. Clin. North Am.* **50**, 523–545 (2021).
25. Villanueva-Millan, M. J. *et al.* Hydrogen sulfide producers drive a diarrhea-like phenotype and a methane producer drives a constipation-like phenotype in animal models. *Dig. Dis. Sci.* **69**, 426–436 (2024).
26. FDA. FDA approves two therapies to treat IBS-D [news release]. Silver Spring, MD, 2015.
27. Rezaie, A. *et al.* Lactulose breath testing as a predictor of response to rifaximin in patients with irritable bowel syndrome with diarrhea. *Am. J. Gastroenterol.* **114**, 1886–1893 (2019).
28. Aslam, S. & Darouiche, R. O. Role of antibiofilm-antimicrobial agents in controlling device-related infections. *Int. J. Artif. Organs* **34**, 752–758 (2011).

Author contributions

Conceptualization: MP, RM; Formal analysis: GL, AR, MP; Funding acquisition: MP, GMB; Investigation: GL, WM, JFG, GP, MLP, GMB, MJVM, MS, SA, SW, AR, MP; Methodology: GL, WM, SW, MP; Project administration: RM, MP; Supervision: WM, SW, RM, MP; Visualization: GL; Writing—original draft: GL, GMB, WM, MP; Writing—review & editing: GL, GMB, WM, AR, RM, MP.

Funding

The authors would like to thank the following donors for their support: The Scott Gray Donor Advised Fund, the Gottesdiener Foundation, the Tull Family Foundation, Thomas Wurster and David Allen, and the DiCecco Family Foundation. These sponsors played no role in the study design or in the collection, analysis, and interpretation of data.

Competing interests

M.P. is a consultant for Ferring Pharmaceuticals Inc., Salvo Health, Dieta Health and Vivante Health Inc. A.R. is a consultant/speaker for and has received grant support from Bausch Health. Cedars-Sinai has a licensing agreement with Gemelli Biotech and Hobbs Medical. A.R., M.P., and R.M. have equity in Gemelli Biotech and Good LFE. M.P. has equity in Dieta Health, Salvo Health and Vivante Health. All other authors report no competing interests.

Additional information

Correspondence and requests for materials should be addressed to M.P.

Reprints and permissions information is available at www.nature.com/reprints.

Publisher's note Springer Nature remains neutral with regard to jurisdictional claims in published maps and institutional affiliations.

Open Access This article is licensed under a Creative Commons Attribution-NonCommercial-NoDerivatives 4.0 International License, which permits any non-commercial use, sharing, distribution and reproduction in any medium or format, as long as you give appropriate credit to the original author(s) and the source, provide a link to the Creative Commons licence, and indicate if you modified the licensed material. You do not have permission under this licence to share adapted material derived from this article or parts of it. The images or other third party material in this article are included in the article's Creative Commons licence, unless indicated otherwise in a credit line to the material. If material is not included in the article's Creative Commons licence and your intended use is not permitted by statutory regulation or exceeds the permitted use, you will need to obtain permission directly from the copyright holder. To view a copy of this licence, visit <http://creativecommons.org/licenses/by-nc-nd/4.0/>.

© The Author(s) 2024